

**AD-A190 810**

**DTIC FILE COPY**

# **CHARACTERIZATION AND MODELING OF THORACO-ABDOMINAL RESPONSE TO BLAST WAVES**

## **Volume 1. Project Summary**

**Annual/Final Report**

**May 1985**

*\*Original contains color  
plates: All DTIC reproductions  
will be in black and  
white\**

**J. H. Stuhmiller  
Principal Investigator**

**JAYCOR  
11011 Torreyana Road  
San Diego, California 92121**

**Contract No. DAMD17-82-C-2062**

**Supported by**

**U. S. Army Medical Research and Development Command  
Fort Detrick, Frederick, Maryland 21701**

**Approved for public release; distribution unlimited**

**DTIC  
ELECTE  
FEB 16 1986  
S D**

**88 2 12 055**

The findings in this report are not to be construed as an official Department of the Army position unless so designated by other authorized documents.

Accession For	
NTIS CRA&I	<input checked="checked" type="checkbox"/>
DTIC TAB	<input type="checkbox"/>
Unannounced	<input type="checkbox"/>
Justification	
By	
Distribution/	
Availability Codes	
Dist	Avail. and/or Special
A-1	



## REPORT DOCUMENTATION PAGE

Form Approved  
OMB No. 0704-0188

1a. REPORT SECURITY CLASSIFICATION UNCLASSIFIED		1b. RESTRICTIVE MARKINGS	
2a. SECURITY CLASSIFICATION AUTHORITY		3. DISTRIBUTION/AVAILABILITY OF REPORT Approved for public release; distribution unlimited	
2b. DECLASSIFICATION/DOWNGRADING SCHEDULE		5. MONITORING ORGANIZATION REPORT NUMBER(S)	
4. PERFORMING ORGANIZATION REPORT NUMBER(S)		7a. NAME OF MONITORING ORGANIZATION	
6a. NAME OF PERFORMING ORGANIZATION JAYCOR	6b. OFFICE SYMBOL (if applicable)	7b. ADDRESS (City, State, and ZIP Code)	
6c. ADDRESS (City, State, and ZIP Code) 11011 Torreyana Road San Diego, California 92121		9. PROCUREMENT INSTRUMENT IDENTIFICATION NUMBER DAMD17-82-C-2062	
8a. NAME OF FUNDING/SPONSORING ORGANIZATION U.S. Army Medical Research & Development Command	8b. OFFICE SYMBOL (if applicable)	10. SOURCE OF FUNDING NUMBERS	
8c. ADDRESS (City, State, and ZIP Code) Fort Detrick Frederick, Maryland 21701-5012		PROGRAM ELEMENT NO. 61102A	PROJECT NO. 3M1 61102BS10
		TASK NO. CG	WORK UNIT ACCESSION NO. 087
11. TITLE (Include Security Classification) (U) Characterization and Modeling of Thoraco-Abdominal Response to Blast Waves Volume 1, Project Summary			
12. PERSONAL AUTHOR(S) James H. Stuhmiller			
13a. TYPE OF REPORT Annual/Final	13b. TIME COVERED FROM 2/15/82 TO 5/31/85	14. DATE OF REPORT (Year, Month, Day) 1985 May	15. PAGE COUNT 46
16. SUPPLEMENTARY NOTATION Annual covers time period of 15 February 1984 - 31 May 1985. Annual/Final published in 8 volumes			
17. COSATI CODES		18. SUBJECT TERMS (Continue on reverse if necessary and identify by block number)	
FIELD	GROUP	SUB-GROUP	
06	21		
06	17		
19. ABSTRACT (Continue on reverse if necessary and identify by block number)			
20. DISTRIBUTION/AVAILABILITY OF ABSTRACT <input type="checkbox"/> UNCLASSIFIED/UNLIMITED <input checked="" type="checkbox"/> SAME AS RPT. <input type="checkbox"/> DTIC USERS		21. ABSTRACT SECURITY CLASSIFICATION Unclassified	
22a. NAME OF RESPONSIBLE INDIVIDUAL Mary Frances Bostian		22b. TELEPHONE (Include Area Code) 301-663-7325	22c. OFFICE SYMBOL SGRD-RMI-S



2 February 1988

2263

Defense Technical Information Center (DTIC)  
Attn: DTIC-DDAC  
Cameron Station  
Alexandria, VA 22304-6145

Subject: Final Report for Contract No. DAMD17-82-C-2062, Volumes 1 through 8

Gentlemen:

Enclosed are 11 copies of each volume of the subject report plus one original of each volume for reproduction. Please return the originals after processing to:

Patricia A. Faller  
Applied Science and Engineering Technology Group  
JAYCOR  
P. O. Box 85154  
San Diego, CA 92138-9259

Phone: [619] 453-6580, ext. 213

Respectfully,

A handwritten signature in cursive script, reading "Pat Faller". The signature is written in dark ink and is positioned below the typed name.

Patricia A. Faller  
Technical Editor  
Applied Science and Engineering Technology Group

pf

Encl.

## **FOREWORD**

This Annual/Final Report has eight volumes. The titles are as follows:

1. Project Summary
2. Elast Load Definition on a Torso Model
3. Lung Dynamics and Mechanical Properties Determination
4. Biomechanical Model of Thorax Response to Blast Loading
5. Experimental Investigation of Lung Injury Mechanism
6. Biomechanical Model of Lung Injury Mechanisms
7. Gastrointestinal Response to Blast
8. Effect of Clothing on Thoracic Response

## CONTENTS

	<u>Page</u>
INTRODUCTION .....	1
BIOENGINEERING APPROACH .....	3
OBJECTIVES .....	6
PUBLICATIONS .....	7
SUMMARY OF RESULTS .....	9
BLAST LOAD DISTRIBUTION .....	9
STRUCTURAL AND MATERIAL DESCRIPTION .....	13
MATERIAL PROPERTIES DETERMINATION .....	23
THORACIC RESPONSE .....	25
LUNG INJURY MECHANISMS .....	34
EFFECTS OF CLOTHING .....	39



## ILLUSTRATIONS

	<u>Page</u>
1. Causal connection between blast environment and damage .....	5
2. Model geometry, probe locations and blast overpressure incidence angle .....	10
3. Variation of peak pressure distribution around the torso model .....	11
4. Comparison of normalized impulse loadings for $\theta = 0^\circ$ .....	12
5. Pressure contours as calculated by the EITACC gas dynamics code for the case of an incident wave of peak 3.4 psi oriented at $30^\circ$ to the chest wall .....	14
6. Comparison of calculated and measured pressure signals for free field and probes .....	15
7. Comparison of calculated and measured peak pressures .....	16
8. Comparison of calculated and measured impulses .....	17
9. Sheep torso model (head up posture) .....	19
10. Influence of abdominal air on ITP responses .....	21
11. Two-dimensional cross-sectional thorax model based on anatomical view .....	22
12. Bulk modulus of lung tissue and bulk modulus of whole lung .....	24
13. Suddenly applied stresses were used to determine viscoelastic properties .....	26
14. Sensitivity studies have shown which material properties are important for <u>gross</u> motion and ITP .....	28
15. Comparison of predicted intrathoracic pressure and measured esophageal pressure for a single peak blast due to a 16 lb TNT charge .....	30
16. Comparison of predicted intrathoracic pressure and measured esophageal pressure for an exposure to two 40 psi blast waves separated in time by 7.6 msec .....	31
17. Comparison of predicted intrathoracic pressure and measured esophageal pressure for an exposure to two 40 psi blast waves separated in time by 9.7 msec .....	32



	<u>Page</u>
18. Dynamic loading on one side of the lung produced direct measurement of wave speed .....	33
19. Observed distribution of injury .....	35
20. Iso-impulse study comparison of the FEM model prediction with WRAIR experimental results .....	37
21. Weight gain in an isolated lung increases rapidly where the peak pressure of a directly applied blast wave exceeds 2.0 psi .....	38

## INTRODUCTION

Death and severe injury from blast exposure has been a workplace hazard since the first use of high explosives in mining. Transport of combustible fuels and the manufacture of almost every petrochemical are modern day additions to this risk. The design of most industrial systems concentrates on the prevention and containment of explosion, so that little is known about the level of exposure that is injurious.

Interest in the lethality of the blast following a nuclear explosion prompted several animal studies in the 1960's that did identify the circumstances in which death would occur. There was no need to define the conditions of incipient or chronic injury, however, the results clearly showed that the soft, air-filled organs (lungs, gastro-intestinal tract, larynx, and tympanic cavities) are damaged.

In the past decade there has been renewed interest by the U.S. Army in blast injury, now at occupational exposure levels. Several weapon systems, notably self-propelled howitzers and shoulder-fired anti-tank rounds, are of such power that the crews and troops using them are exposed to pressure fields of unprecedented magnitude. Although it is certain that such exposures are not associated with acute injury, they do approach the exposure limits set by military standards. The limits are based on experience with safe conditions, rather than on known injury thresholds. To extend these boundaries for training purposes, it is necessary to establish that subtle or chronic injury will not occur.

A common procedure for determining human risk is to make comparison with similar animal exposure. The uncertainty of this procedure arises from the extrapolation of results between species. Body weight, size, orientation, internal organ arrangement, and other anatomical factors must be considered in interpreting test results. Furthermore, large numbers of animal must be used to produce statistically significant averages and to overcome variations in individual animals. As the number of blast conditions to be studied increases, the total number of animals, as well as the cost and duration of the testing, grows dramatically.

One way of reducing the amount of animal testing required is to use mathematical models. In the simplest applications, mathematics is used to fit a smooth curve through some test conditions in order to extend the results to other conditions. This approach may not correctly predict results outside of the range already tested and cannot address extrapolation to other species.

A more satisfactory model results from incorporating the mechanics of the process and physiology of the animal. Such a model was proposed as an adjunct to the animal testing at the Lovelace Inhalation Toxicology Research Institute (ITRI). The lung was represented by a gas-filled volume, the chest wall by a piston, and the rigidity of the skeletal system by an opposing spring. When the pressure history of the blast wave is applied to the external surface of the piston, the piston accelerates inward, compressing the gas until it is finally brought to rest by the combined action of the gas pressure and the force of the spring. The various parameters of the model were calibrated to reproduce the peak internal pressures seen in the test animals. It was also proposed that the parameters would scale with total body mass of the animal according to certain geometric rules.

This model is able to correlate, and to some extent explain, a limited range of internal pressure data for simple waves. In fact, it has been the only model of thoracic response to blast used. Still, it is not capable of answering the hazard questions discussed earlier. First of all, the parameters of the model are not directly related to measurable physiological properties, instead they have been chosen to give the best agreement with internal pressure data. Therefore, although one may speculate as to their origin, one cannot confidently judge how they would change between species. Secondly, there is no connection made with the mechanism of injury. While large internal pressures undoubtedly indicate a more hazardous environment, the location and severity of injury cannot be inferred from such a model.

There is another kind of model of the thorax that has taken the physiological details into account. Borrowing from the techniques of structural engineers, detailed models of the skeletal system of the chest have been produced that use measurable, mechanical properties of the bone and incorporate all of the connections and linkages. These models have been quite successful in studying the blunt trauma of automobile crashes, where the body is

thrown into a solid object. The injury of interest in a crash is bone fracture, so that no modeling of the soft tissue is included. In blast exposure, on the other hand, skeletal deformation is relatively small and serves only to transmit motion to the compliant organs inside where the damage process takes place. Therefore, although the ambiguity of the description is removed, the models do not address the problem of interest.

The work summarized in this report has expanded upon these ideas to construct a model of the thorax that contains a structural description of the hard and soft tissues. Supplemented with field measurements of load distribution and laboratory measurements of tissue properties, the model predicts the detailed motion of the thorax and indicates the magnitude and distribution of damage.

#### **BIOENGINEERING APPROACH**

To understand how engineering techniques can be used to determine injury to a biological system, it is instructive to consider an analogous situation of determining under what meteorological conditions a bridge would be damaged.

First, the mechanical process would be broken down into a series of causal events : (1) the winds and pressures of the weather system exert forces on the bridge; (2) the structure of the bridge distorts under these loads and produces internal stresses; and (3) when the internal stresses exceed the strength of the material, the bridge fails.

With the overall chain of events established, then each link can be developed. The loading depends on the magnitude, duration, and direction of the wind, and on the shape of the bridge. The load distribution would be determined through a combination of small, scaled tests in a wind tunnel, calculations solving the appropriate gas dynamics equations, and final verification against measurements made on an actual bridge of interest (during less hazardous conditions). Similarly, the distortion of the bridge depends upon the distribution of the load, its particular structural type, and the material from which it is constructed. Again model tests and structural analysis would be confirmed by actual measurements on a bridge. Finally, the strength of the bridge material would be determined in laboratory tests in which the material was stressed until it failed.

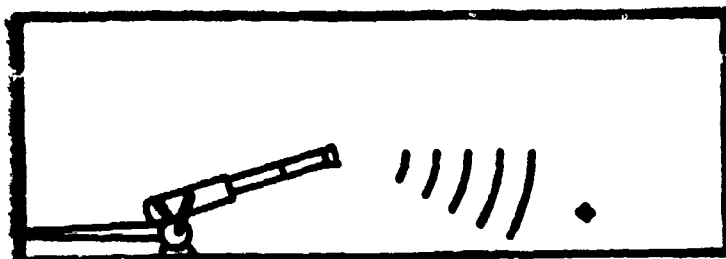
Having completed the description for one particular type of bridge, verifying each of the causal links separately and confirming the final prediction of failure against an instance where damage did occur, the collection of models could be applied with some confidence to determining the possibility of hazard in other, untested situations. The effects of different wind fields, bridge design, and material properties can all be systematically accounted for with a minimum of additional testing and without the need to subject a real bridge to damage in order to develop empirical data.

The same approach can be applied to a biological system exposed to blast. A series of causal links can be established that translate the blast conditions into load, motion, and tissue stress. The material strength of the various organs determines their susceptibility and mode of injury. Verification can be based on animal tests and then confidently extended to man and to other environments that have not been tested.

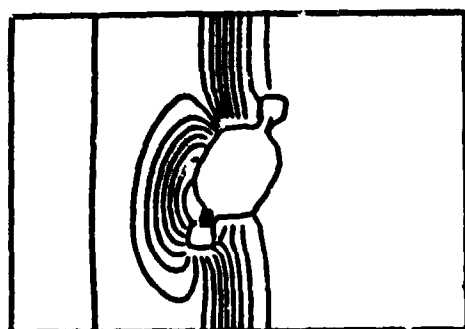
The causal connection between blast and injury is illustrated in Figure 1. The blast wave, created by the weapon, reflects and evolves as it propagates to the location of interest. There it strikes the body and produces a load distribution that depends on body shape, orientation, and perhaps clothing. This external loading sets the body in motion which produces rapidly changing internal stresses. Those internal stresses are concentrated by geometric features and at the boundaries between dissimilar materials. When the local stresses exceed a certain threshold value, failure of the tissue and blood vessels result in observable injury.

Figure 1 also indicates that for each step in the chain of events, there is a quantity that can measure the result of the process and provide a separate test of each component model. It is this separate verification that gives confidence to the overall model when it is applied to a new situation. Conversely, the nature of the linkage suggests measurements that will specifically test the underlying concepts.

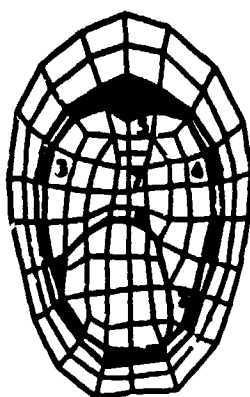
The steps leading to the determination of local tissue stress have a one-to-one correlation with the bridge analogy mentioned earlier and therefore the same approach is likely to be successful. To have confidence that stress can be related to injury, we must know that there is an equally strong analogy



High pressure waves created by weapon reflect and evolve as they propagate to the crew location.



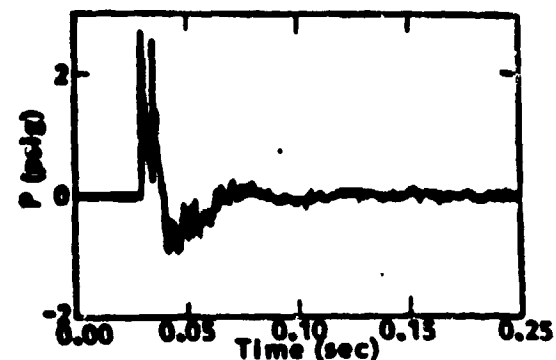
The blast wave interacts with the body producing a loading that depends on body shape and orientation.



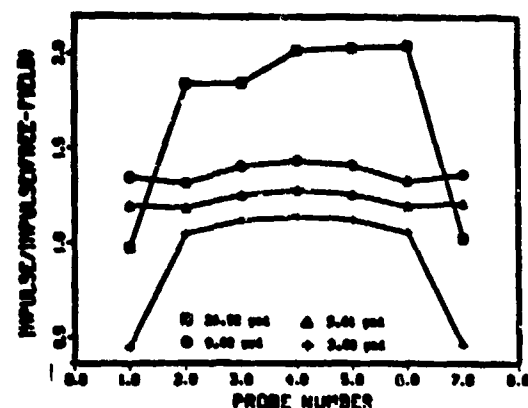
The external loading sets the body in motion causing rapid changes in internal stress.



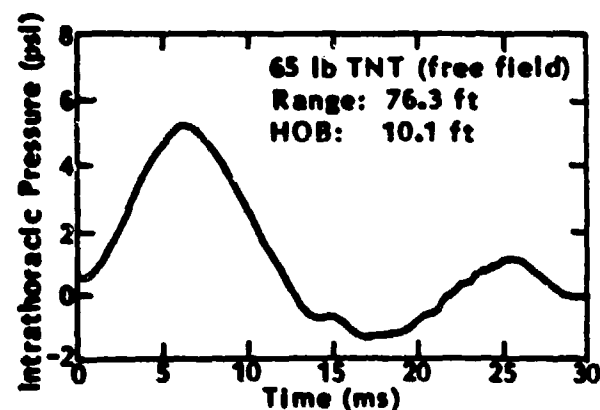
Local stress concentrations cause mechanical failure of tissue and blood vessels resulting in injury.



Observed free-field pressure history.



Observed load distribution.



Observed intrathoracic pressure.



Observed injury.

Figure 1. Causal connection between blast environment and damage.

between the failure of ordinary materials and the characteristics of injury we want to capture. Several such examples exist.

The observation that injury increases with blast strength and that there is a threshold level for injury is certainly described by the concept of a material failure stress level observed in all materials. A second observation of animal tests is that the threshold for injury is less for repeated exposures. This behavior parallels fatigue failure in which the material is damaged a little on each stressing until the cumulative damage leads to failure (for example, bending a paper clip repeatedly). Direct evidence of this explanation would be revealed in material property changes to the organ. Finally, there is some evidence that blast waves in rapid succession can produce injury that is different from the same number of repeated exposures. Again, there is an analogous situation for other materials in which their properties change momentarily under large stress and require a certain characteristic time to recover to their nominal values. If they are subjected to additional stress before they can recover, they may be more or less susceptible to damage.

These analogies between engineering situations that have been successfully described by mechanistic concepts and the aspects of blast injury that must be quantified to develop occupational level safety criteria are the source of guidance in the modeling program. The remainder of this report describes the progress that has been made to develop, verify, and use these concepts.

## OBJECTIVES

Based on these concepts, <sup>This</sup> a project was initiated by the U.S. Army Medical Research and Development Command under the technical direction of the Department of Respiratory Research, Walter Reed Army Institute of Research (WRAIR) to develop analytical methods to determine the body's response to blast wave loading. The primary emphasis was placed on occupational level exposure and on the lung as the threatened organ. The goal was to identify those aspects of the blast field that can be correlated with injury observed in animals. Secondary emphasis was placed on identification of the specific injury mechanisms in the lung, determination of stress distribution in viscera such as the trachea, and extension of the results to complex wave environments. → cont'd pg 7

Copy  
Fung 6

During the course of the work, the gastrointestinal tract took on more importance as a target organ and a separate experimental effort was initiated. By the end of the project, complex waves within vehicles became a concern, but data describing the phenomena had not been released. In addition, field studies showed increased intrathoracic pressure response for subjects wearing ballistic jackets, so an additional study task was added to quantify the change in body loading. Keywords: mathematical models, anatomical models, weapons effects, occupational diseases, exposure (physiology) ←

## PUBLICATIONS

The work was carried out by a team of researchers both at JAYCOR and at the University of California, San Diego. The detailed progress of that work was documented in topical reports that are presented as volumes to this final report. They are:

- Vol. 2 "Blast load definition on a torso model"
- Vol. 3 "Lung dynamics and mechanical properties determination"
- Vol. 4 "Biomechanical model of thorax response to blast loading"
- Vol. 5 "Experimental investigation of lung injury mechanisms"
- Vol. 6 "Biomechanical model of lung injury mechanisms"
- Vol. 7 "Gastrointestinal response to blast"
- Vol. 8 "Effects of clothing on thorax response"

In addition, several papers were prepared for publication in archival journals or for presentation at scientific meetings. They are:

"The Incremental Elastic Moduli of the Lung," M. R. T. Yen, C. Artand, and Y. C. Fung, to be submitted for publication (1985).

"Speed of Stress Wave Propagation in the Lung," M. R. T. Yen, Y. C. Fung and H. H. Ho, AMES/Bioengineering Report No. 85-1, University of California, San Diego (1985).

"Edema of Lung Due to Impact Injury," M. R. T. Yen, Z. L. Tao, and Y. C. Fung, AMES/Bioengineering Report No. 852, University of California, San Diego (1985).

"Thoracic Trauma Study: Rib Markings on the Lung Due to Impact are Marks of Collapsed Alveoli, Not Hemorrhage," M. R. T. Yen and Y. C. Fung, AMES/Bioengineering Brief Note, University of California, San Diego, (198\_).

"Simulation of Thoracic Responses to Blast Waves - A Finite Element Approach," C. J. Chuong and J. H. Stuhmiller, presented at the Fourth International Conference on Mechanics in Medicine and Biology, July 8-11, 1984, SUNY/Buffalo, Buffalo, N.Y.



"Computer modeling of thoracic response to blast," J. H. Stuhmiller, C. J. Chuong, K. T. Dodd, Y. Y. Phillips, Fifth International Symposium on Wound Ballistics, Gothenberg, Sweden, June 1985

"Blast effects on major organs systems of the body," J. H. Stuhmiller, NATO symposium on "Blast and Applied Aspects of Noise Induced Hearing Loss," Il Ciocco, Italy, September 1985

In support of the contract, detailed briefings were given to the scientific community at WRAIR as part of the symposium

"An engineering approach to modeling blast trauma"

and to the 1984 Meeting of Research Study Group 6, NATO Panel VIII, AC/243 in Meppen, FRG.

## SUMMARY OF RESULTS

### BLAST LOAD DISTRIBUTION

In order to determine the load distribution on a subject in a blast field, model tests were conducted at ITRI. A cylindrical shape was constructed out of aluminum having the cross section of an "average" man. See Figure 2. Circular cylinders were attached at the sides to represent an "arms down" target. Flush-mounted pressure transducers were placed at seven locations around the "chest" to measure the local load time histories. Tests were conducted with bare charges at various locations to produce blast waves in the vicinity of the model with nominal peak pressures of 3, 5, 9, and 25 psi. The model could be oriented at 30° intervals to the direction of the blast over a range of 0° to 180°.

The data from each test was plotted on a strip chart recorder and later digitized from the hard copy using a digitizer pad. The calibration of the pressure probes before and after testing had an average error of 14%, with some being even greater. There were only a few repeated shots and they showed as much as a 25% variation.

Despite the instrument variations, a definite pattern in the load distribution could be discerned. The pressure signals at all locations had a single peak,  $P_L$ , as did the free field wave,  $P_W$ . The ratio of the peak pressures showed a systematic variation with position and intensity of the blast. See Figure 3. Across the side of the model facing the blast, the pressure ratio was about constant for a particular blast strength, and varied from a value of 2 for the smallest waves to 3 for the strongest waves. This behavior is consistent with the "wave doubling" effect that occurs upon reflection from a solid wall. Along the side facing away from the blast the ratio was between 0.75 and 1.0 for all cases. The extreme points in Figure 3b are data from the "arm pit" region which are not representative.

A similar trend is seen in the distribution of positive load impulse around the body. When normalized by the positive impulse of the incident blast wave, the ratio is nearly constant across the body, varying from 1.0 at low pressure levels to 2.0 for stronger waves. See Figure 4. Evaluation of these effects at other orientations was not made.

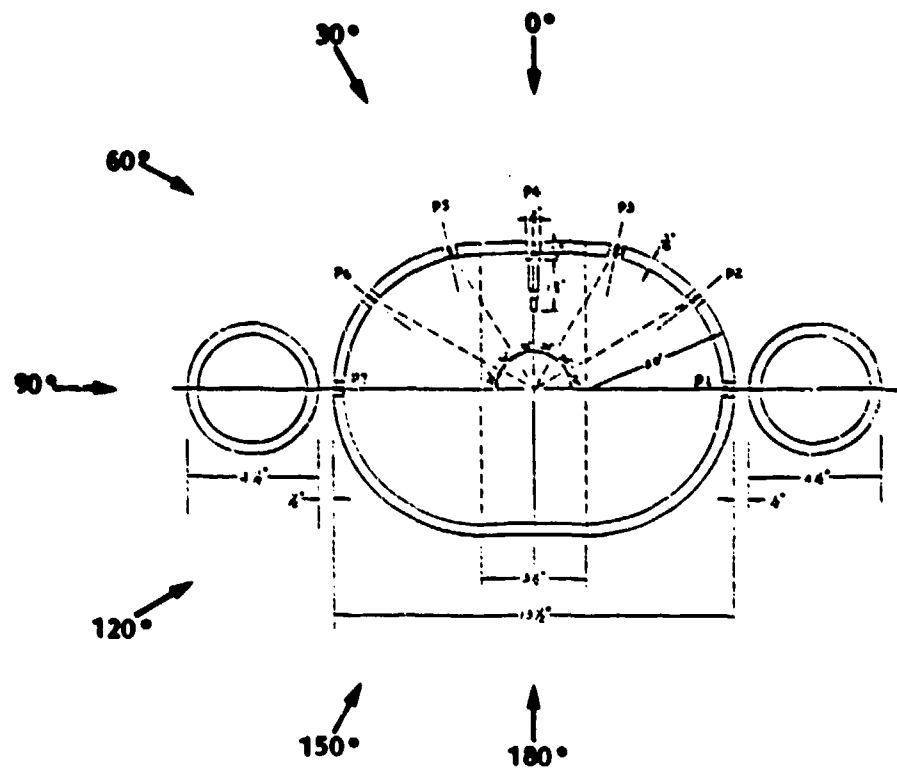
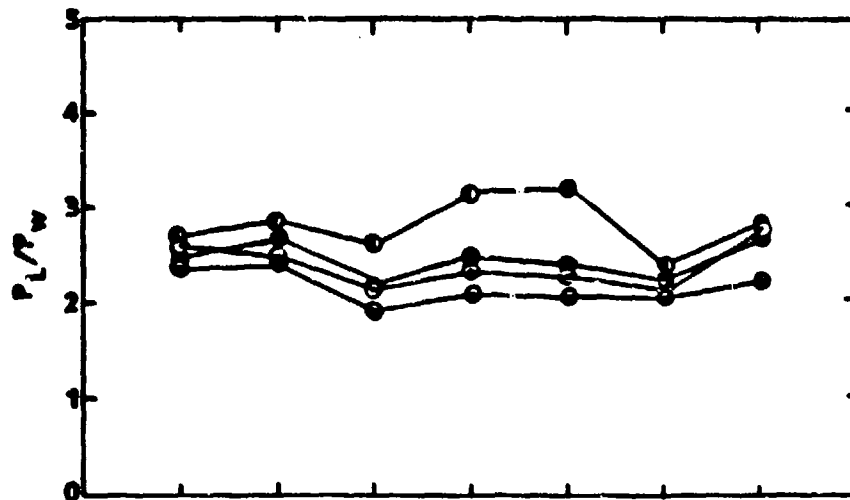
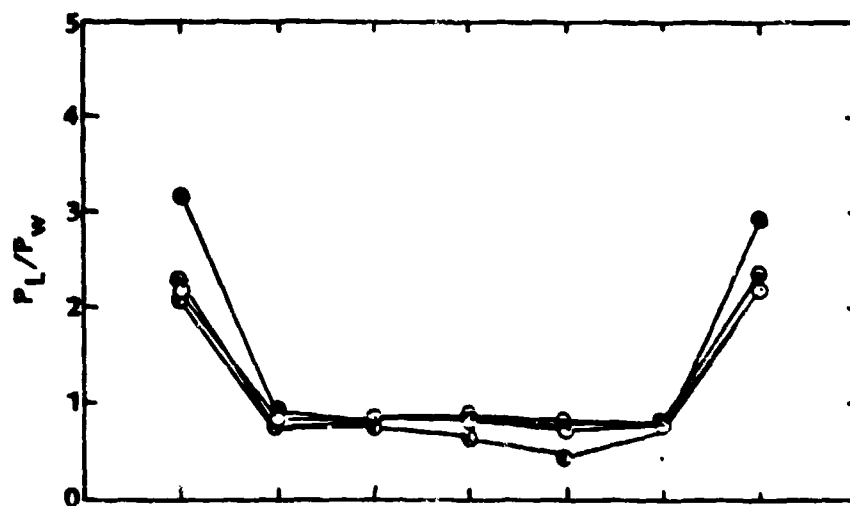


Figure 2. Model geometry, probe locations and blast overpressure incidence angle.



(a) Front



(b) Back

Figure 3. Variation of peak pressure distribution around the torso model (o: 3.85 psi; e: 5.54 psi; e: 8.84 psi; e: 22.31 psi).

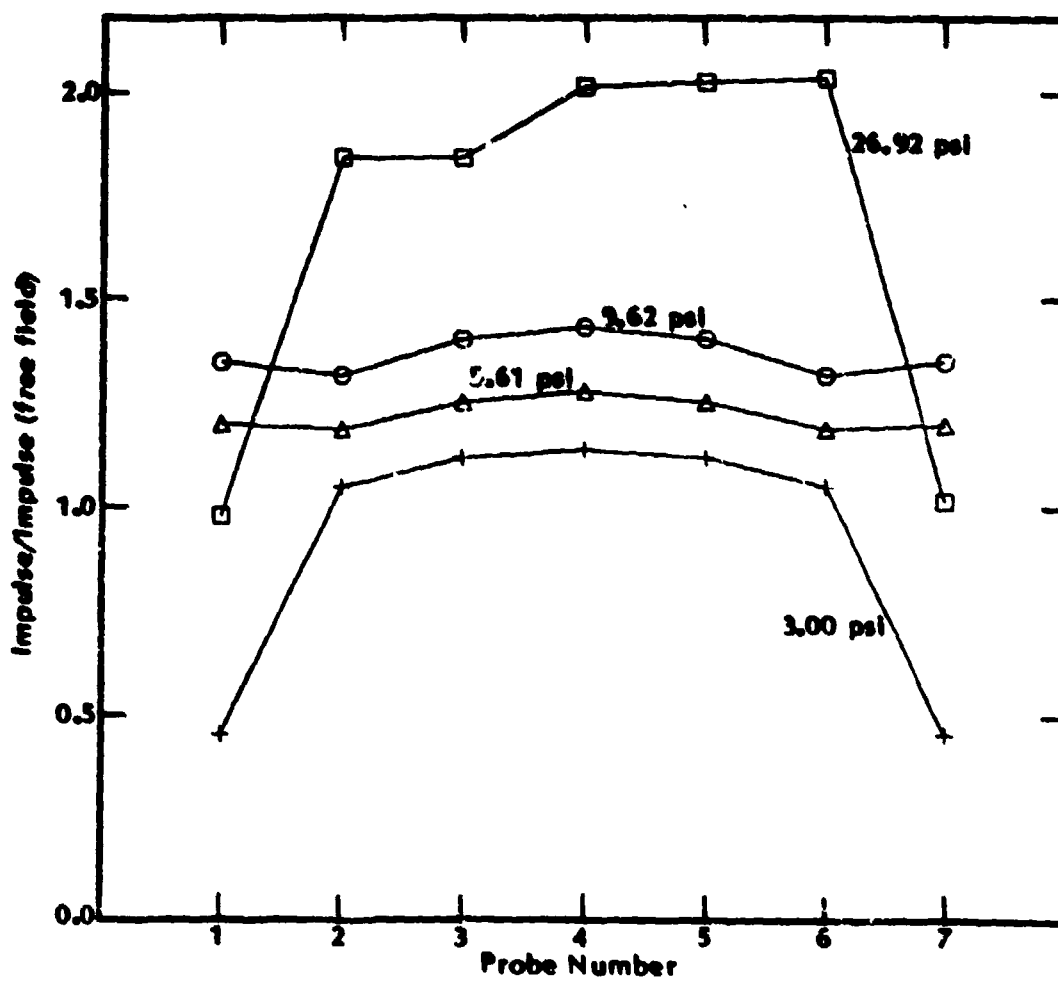


Figure 4. Comparison of normalized impulse loadings for  $\theta = 0^\circ$ .

A few tests were made with the torso model covered with a flannel material called "moleskin". There appeared to be a slight increase in the peak load pressures with the covering. A later study of the effects of clothing explored this phenomenon in greater detail.

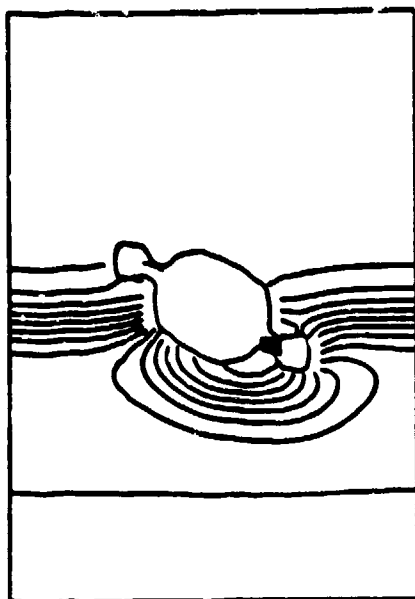
Next, JAYCOR's EITACC computer code for calculating gas dynamic flows was set up for the torso model test geometry. See Figure 5. The code uses finite difference methods to solve the gas dynamics equations of motion in the presence of general body shapes. The calculation is begun at rest and the pressure at the inlet is varied to cause a wave to propagate into the computational region. The wave interacts with the body and eventually passes out of the system. Specially designed boundary conditions allow the wave to leave the finite computational region without spurious reflections.

The computational method was compared with all of the 3 psi wave tests. Figure 6 shows an example. The incident free field wave is shown in the upper left-hand box. The load time histories vary appreciably around the body, with sharply peak, triangular traces on the blast side and broader, squarer traces in the back. The region between the arm and the body has very irregular behavior, probably due to multiple reflections. Overall, the calculation captures the shape of these load histories, even in the arm region. The finite resolution of the mesh used in the calculation limits the temporal resolution that can be reproduced and so the pressure peaks are rounded and the maximum values underpredicted. See Figure 7. When the distribution of positive load impulse is compared, however, the agreement is within the calibration errors of the probes. See Figure 8.

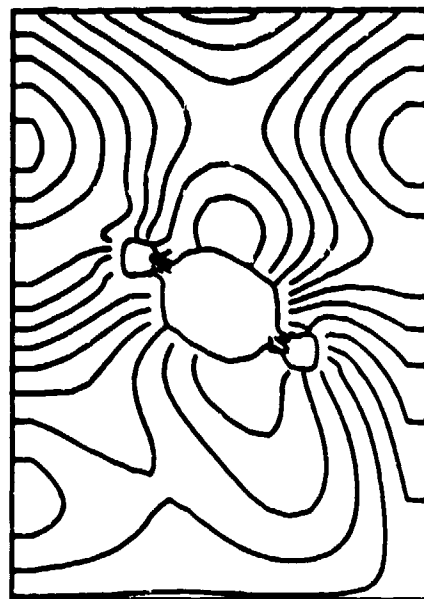
The most important conclusions we have drawn from this work are that load impulse can be a multiple of the free-field impulse, depending on the wave intensity, and that the spatial and temporal distribution of the load can be reasonably predicted by computational models for the occupational level exposures that have been investigated.

#### STRUCTURAL AND MATERIAL DESCRIPTION

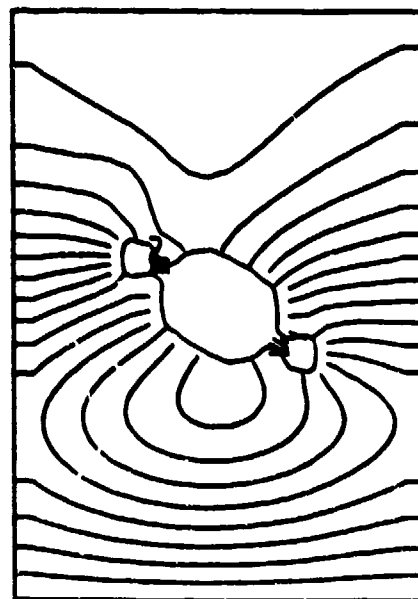
The animal chosen for field test exposures was the sheep. The sheep has a thorax size and construction that is similar to man and has been the test



(a)  $t = 2.00E-3$  sec



(b)  $t = 6.00E-3$  sec



(c)  $t = 10.0E-003$  sec

**Figure 5.** Pressure contours as calculated by the EITACC gas dynamics code for the case of an incident wave of peak 3.4 psi oriented at  $30^\circ$  to the chest wall.

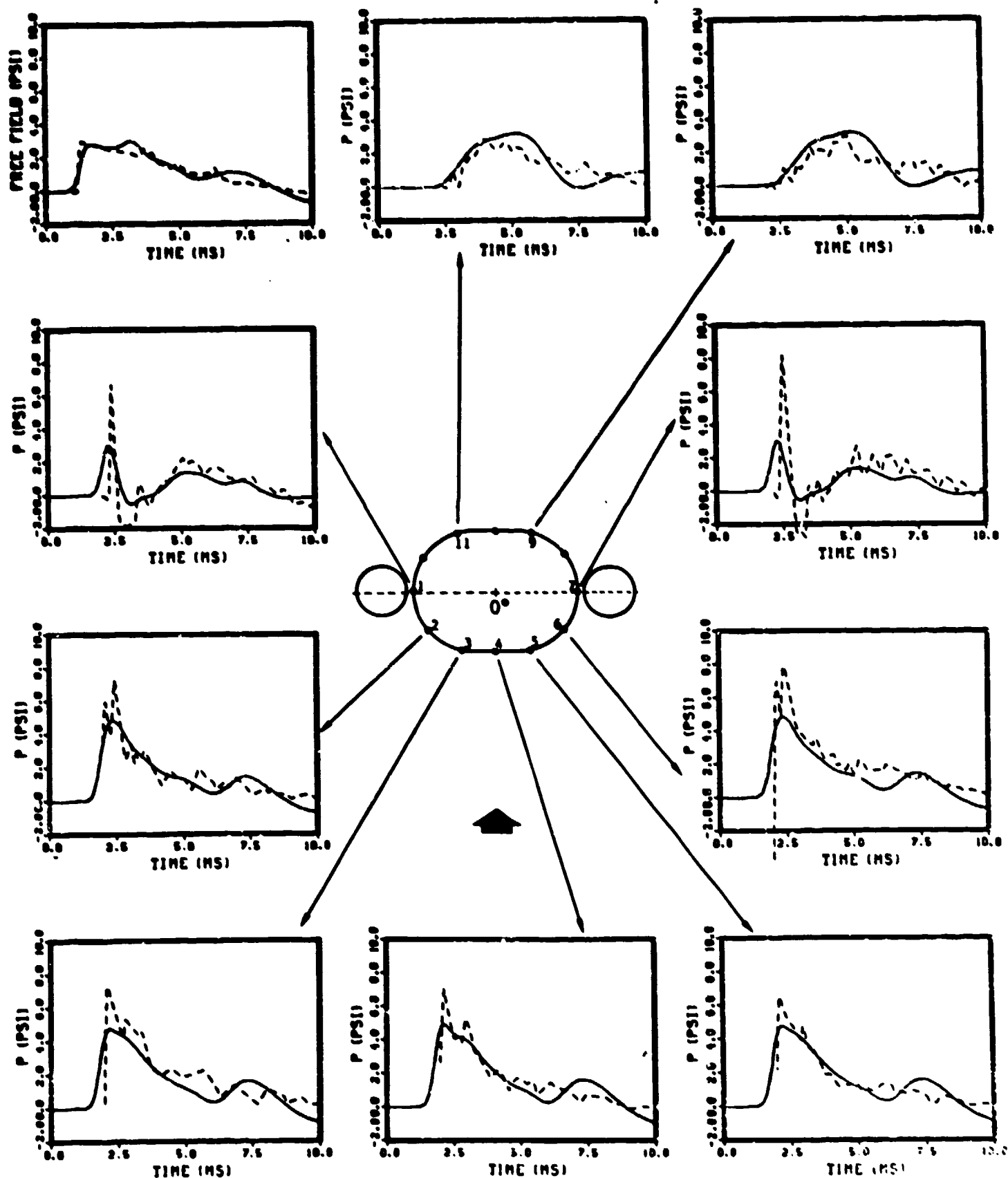
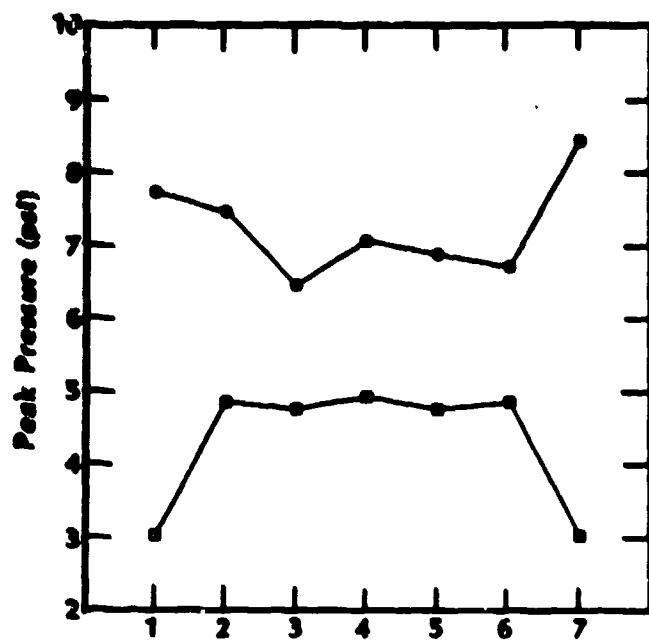
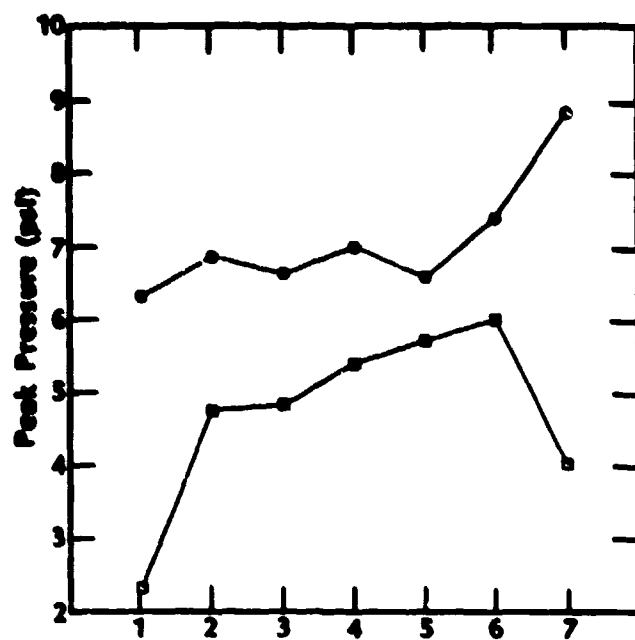


Figure 6. Comparison of calculated (—) and measured (---) pressure signals for free field and probes. 3 psi wave,  $\theta = 0^\circ$ .

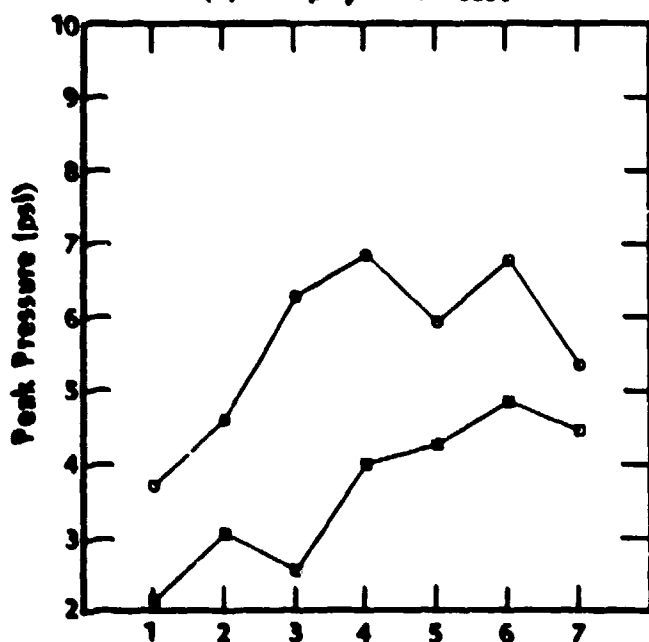




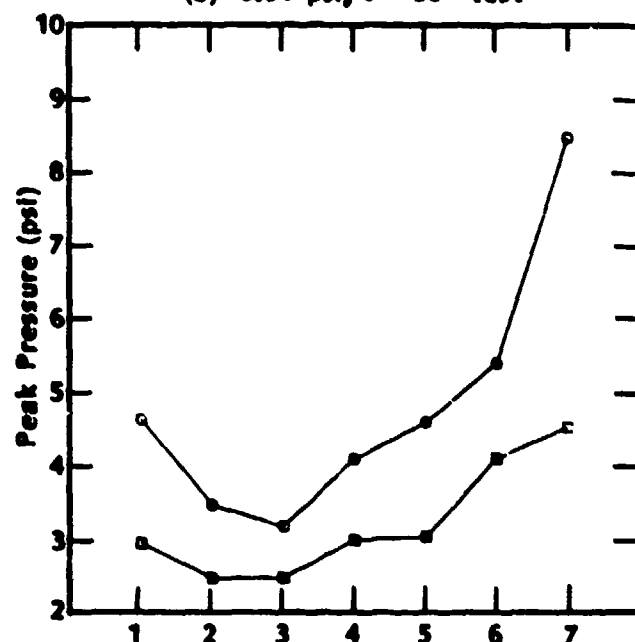
(a) 3.0 psi,  $\theta = 0^\circ$  test



(b) 3.39 psi,  $\theta = 30^\circ$  test

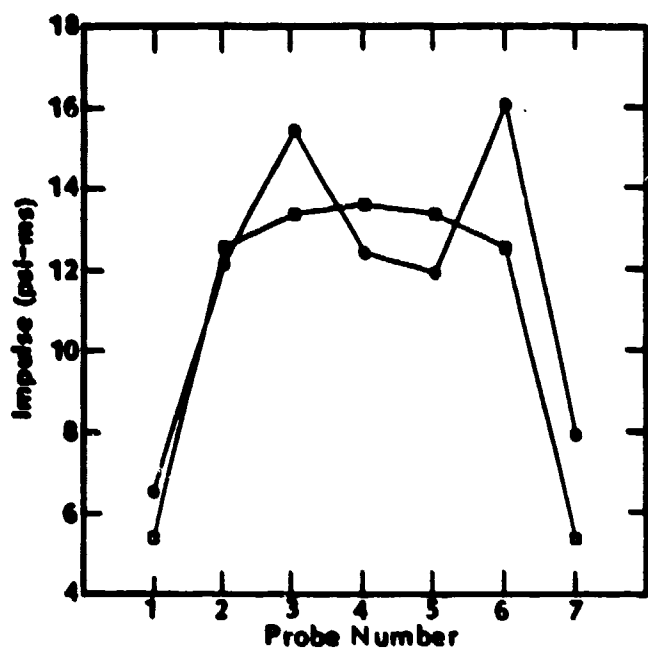


(c) 3.0 psi,  $\theta = 60^\circ$  test

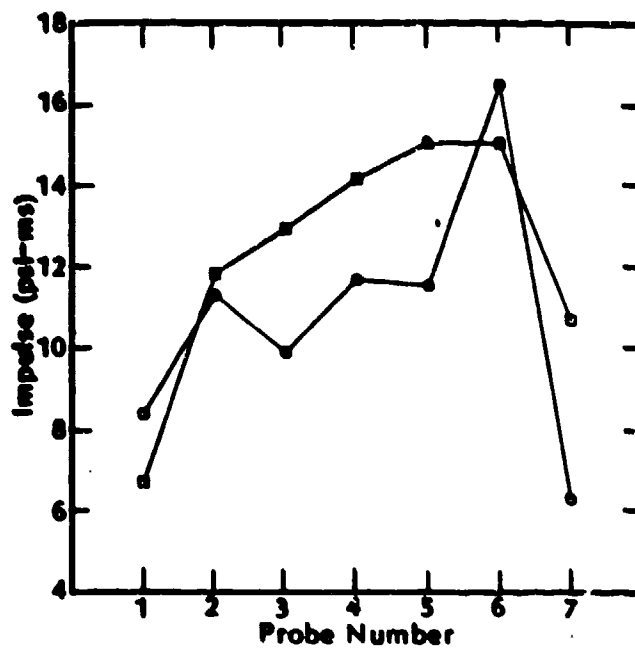


(d) 3.38 psi,  $\theta = 90^\circ$  test

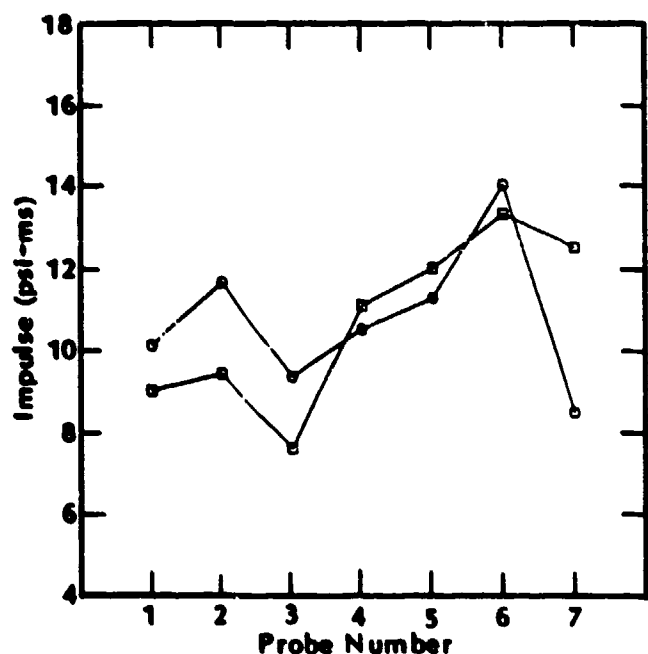
Figure 7. Comparison of calculated (□) and measured (O) peak pressures.



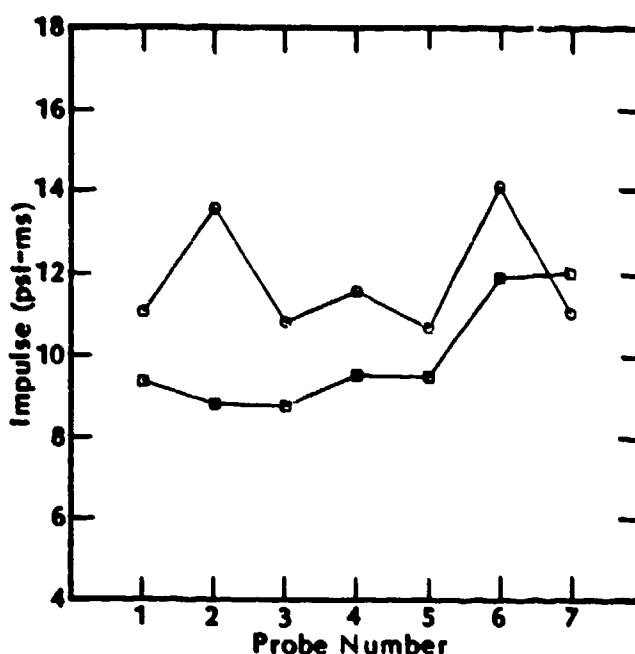
(a) 3.0 psi,  $\theta = 0^\circ$  test



(b) 3.39 psi,  $\theta = 30^\circ$  test



(c) 3.0 psi,  $\theta = 60^\circ$  test



(d) 3.38 psi,  $\theta = 90^\circ$  test

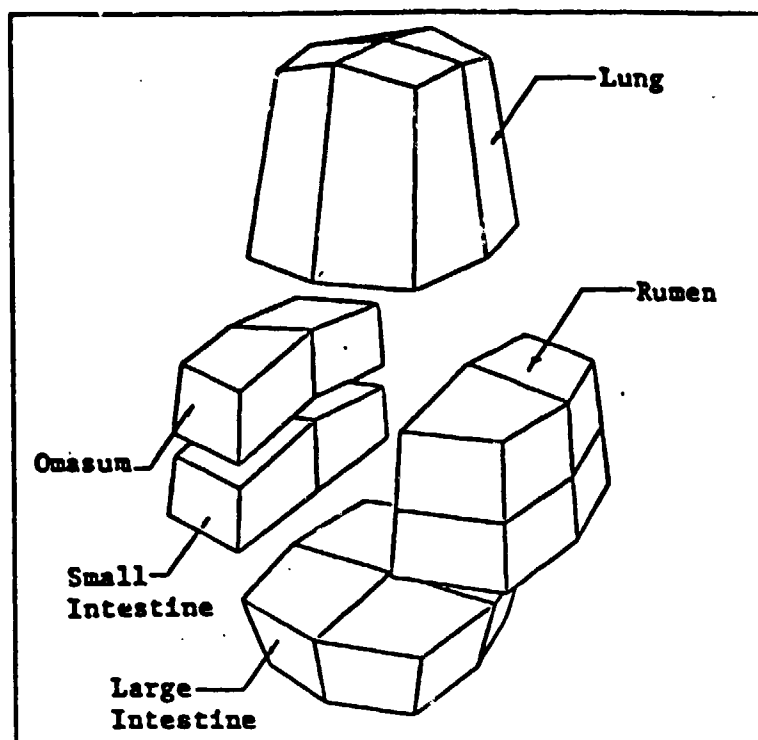
Figure 8. Comparison of calculated (□) and measured (○) impulses.

animal in previous blast investigations so that a body of data already exists. The primary difference is that sheep have large, multiple stomachs that have a considerable air content. It was important to establish early in the investigation what effect this difference might have on the cross-species inferences. The first step in the structural determination was to review the available anatomical literature and select typical dimensions and orientations of organs.

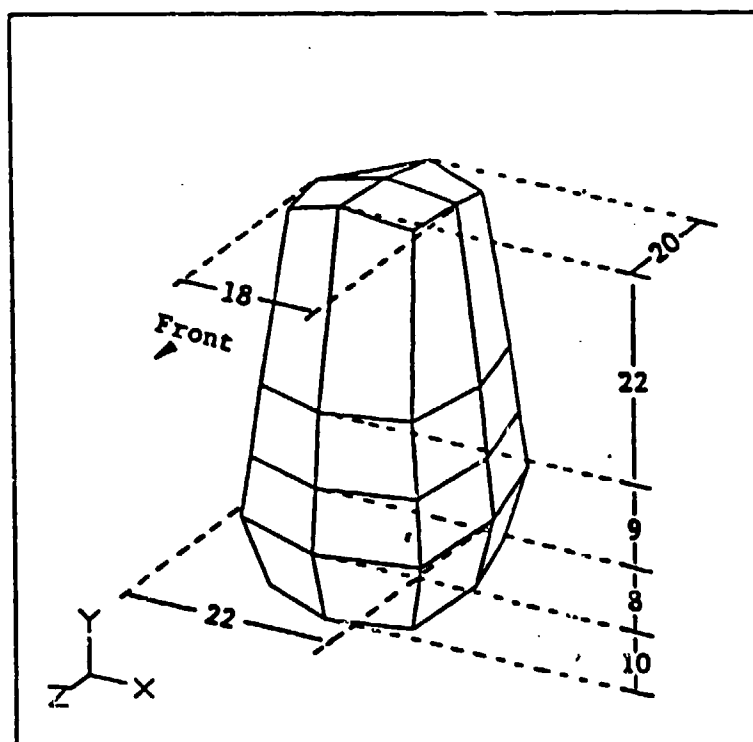
Next, the structural analysis method called finite element modeling was applied. The object to be studied is divided into contiguous blocks, called elements, with shapes that fit natural boundaries. The continuous, differential laws of mechanics are transformed into algebraic equations for the position, velocity, and stress at points within each element. More accuracy (and complexity) results from using more points per element. The properties of the material enter as parameters that are determined by conducting particular experiments. The more complete the description of the material, the more parameters that must be determined. Finally, to advance the model one time step requires solving thousands of equations for thousands of unknowns. There are a variety of numerical algorithms available and a trade-off between cost and accuracy of the solution must be made.

There are four types of choices to make in performing a finite element analysis: size of the element, number of points within the element, complexity of the material description, and the numerical solution technique. For this project we used the FEAP computer code which employs the Newmark method of solution. Each element contained four nodal points with a bilinear interpolation scheme. The material was assumed to be of a linear viscoelastic type, requiring that seven parameters must be determined for each substance. Finally, the size of elements was chosen to be small enough to resolve the phenomena of interest, yet resulting in a mathematical problem that can be solved at reasonable cost.

In order to determine if the gas content of the sheep stomach would significantly influence measurements taken within the thorax, a finite element model was constructed of the entire sheep torso. Three dimensional blocks were used of a size sufficient to capture the major organs. See Figure 9. In this model, the inertia of the rib cage, skeletal muscle, and diaphragm were



(a) Exploded view with various organs represented



(b) Major dimensions of sheep torso model (cm)

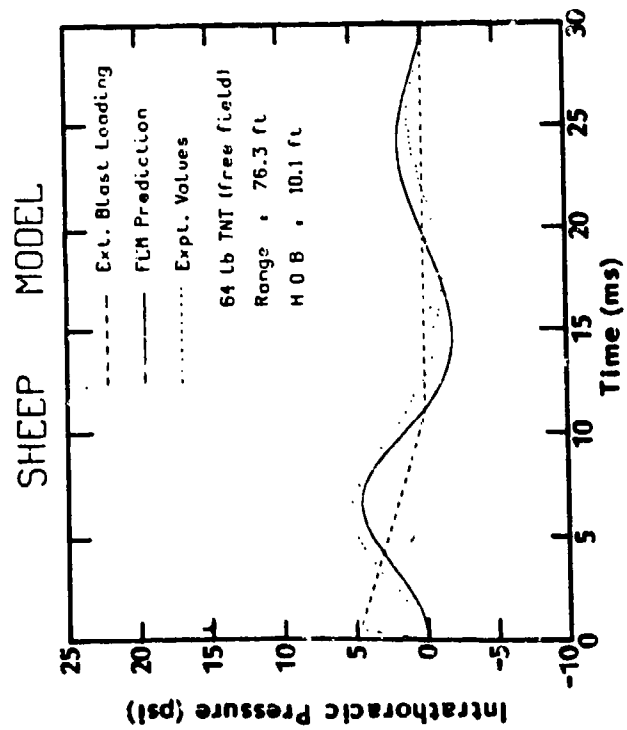
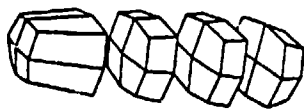
Figure 9. Sheep torso model (head up posture).

incorporated at the appropriate nodal points, thus reducing the number of outer elements required.

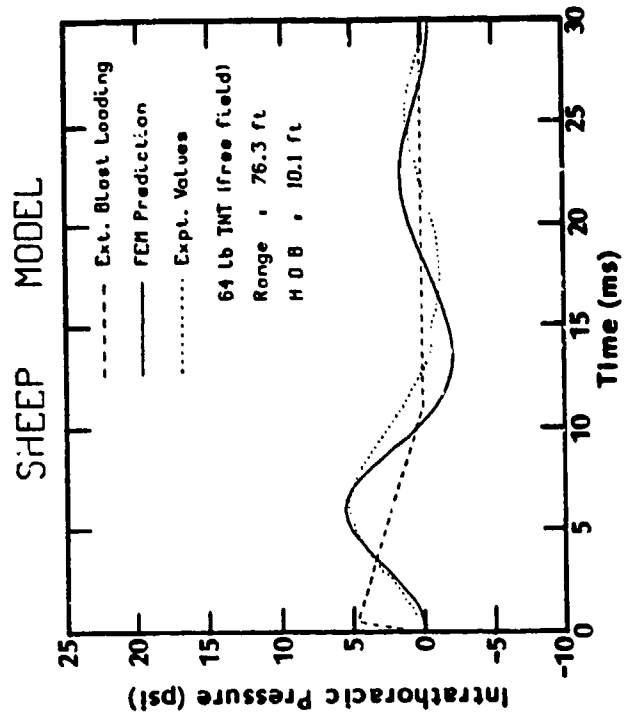
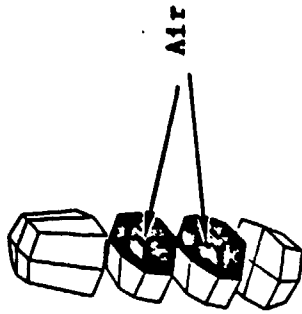
A blast loading, corresponding to cases in which field data was available, was applied to the model surface and the subsequent intrathoracic pressure time histories were compared with data. See Figure 10. Two extreme cases had the rumen filled with all water and with all air. The difference in the prediction was judged to be slight and no greater than that due to uncertainty in the data or material constants. Other calculations using this model, however, showed that the element size was too large to capture the behavior of more rapid events. Based on these results, it was decided to develop a separate thorax model with sufficient resolution to follow the phenomena of interest.

From the earlier collection of anatomical data, a sheep cross-section was selected that corresponds to the approximation location where intrathoracic pressure measurements are made. Based on that view, a two-dimensional finite element model was constructed that captured the geometric arrangement of four distinct parts: skeletal muscle, rib, lung, and a water-filled organ such as the heart. See Figure 11.

There are several approximations that must be taken into account when using and interpreting a two-dimensional representation of a three-dimensional body. First, the motion should be primarily in that plane. Since the thorax of a sheep or man is somewhat cylindrical and since it was previously shown that the motion of the diaphragm has only a small influence on the thorax, this assumption is reasonable. Second, the internal arrangement of the organs varies with the cross-section location and with individual so that the results are only typical, rather than specific. It is likely that intrathoracic pressures, which are taken in a region removed from the lung boundaries, will be less affected by the choice of cross-section. Third, the cross-section view at some locations cuts across the diaphragm, showing thoracic and abdominal organs in the same plane. Since we know these two regions are not strongly connected dynamically, the region has been modeled as an equivalent water-filled (hard to move) organ. Finally, the rib cage adds stiffness to the chest wall through forces that do not originate in the plane being analyzed. Studies were made to determine the best way to include this effect and it was



(a) Model without air in the abdomen



(b) Model with four of the rumen elements replaced by air

Figure 10. Influence of abdominal air on ITP responses.

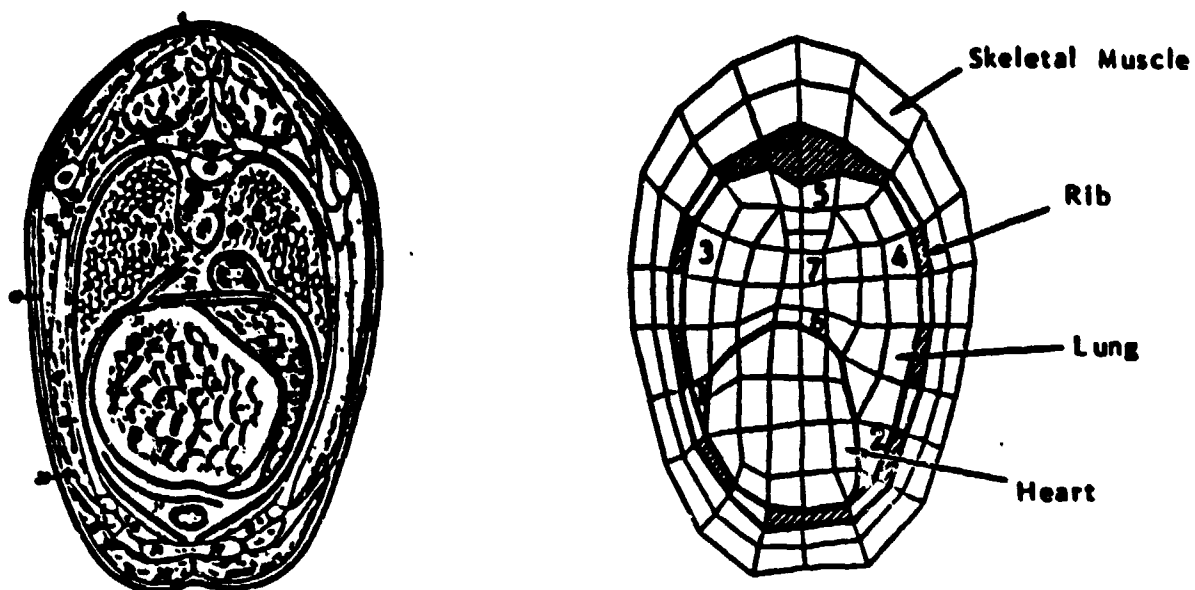


Figure 11. Two-dimensional cross-sectional thorax model based on anatomical view.

concluded that modifying the rigidity of the muscle/bone region to a value intermediate between muscle and bone produced the most satisfactory result. This point is discussed in more detail in the section on thoracic response.

#### **MATERIAL PROPERTIES DETERMINATION**

The properties of the lung parenchyma have the greatest influence on the thorax response, the evolution of intrathoracic pressure, and the nature of damage to the tissue itself. Because of its central role, a special effort was made to determine its properties precisely. The experiments were conducted in the Bioengineering Laboratory at the University of California, San Diego under the direction of Professor Y. C. Fung. There, special instrumentation was used to determine the viscoelastic properties of the lung tissue and of the whole lung, and to conduct dynamic experiments on wave propagation through the parenchyma.

As was mentioned earlier, a linear viscoelastic material model was selected that involves seven material parameters. One parameter is the mass density which is easily measured for the whole lung and changes with inflation. There are two elastic parameters which describe distortions of the material which will fully disappear when the applied stress is removed. One is the bulk modulus,  $K_0$ , which indicates the compressibility of the material, and the other is the shear modulus,  $G_0$ , which indicates the resistance to being bent. Material science has shown that all elastic distortions can be described by combinations of these two effects.

The elastic moduli are found from a combination of the results from two experiments: measurement of the incremental p-V relation and of the force required to produce a small indentation at the lung surface. When the airway is kept open during the p-V tests, the bulk modulus of the tissue is determined; when the airway is closed, the bulk modulus of the entire lung is found. Under blast conditions, the compressions occur so rapidly that little air flow can develop and the lung behaves as though the airway was closed. The  $K_0$  for the tissue alone varies from 20-120 cm H<sub>2</sub>O depending on transpulmonary pressure, while that of the whole lung varies from 1300-1400 over the same range. See Figure 12. This latter variation is of the same order of magnitude as the  $K_0$  for air itself, indicating that the gross properties of the



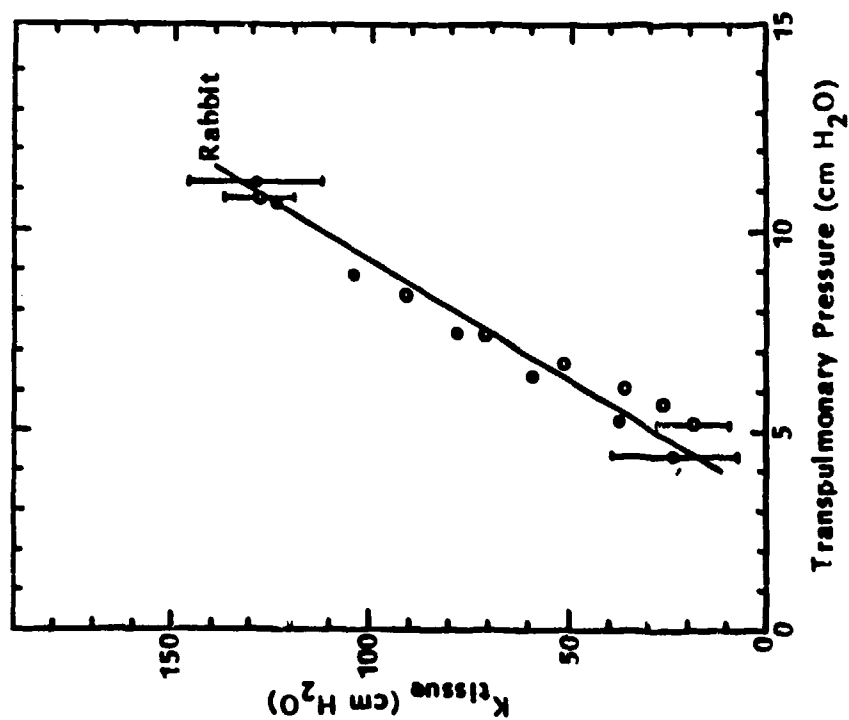
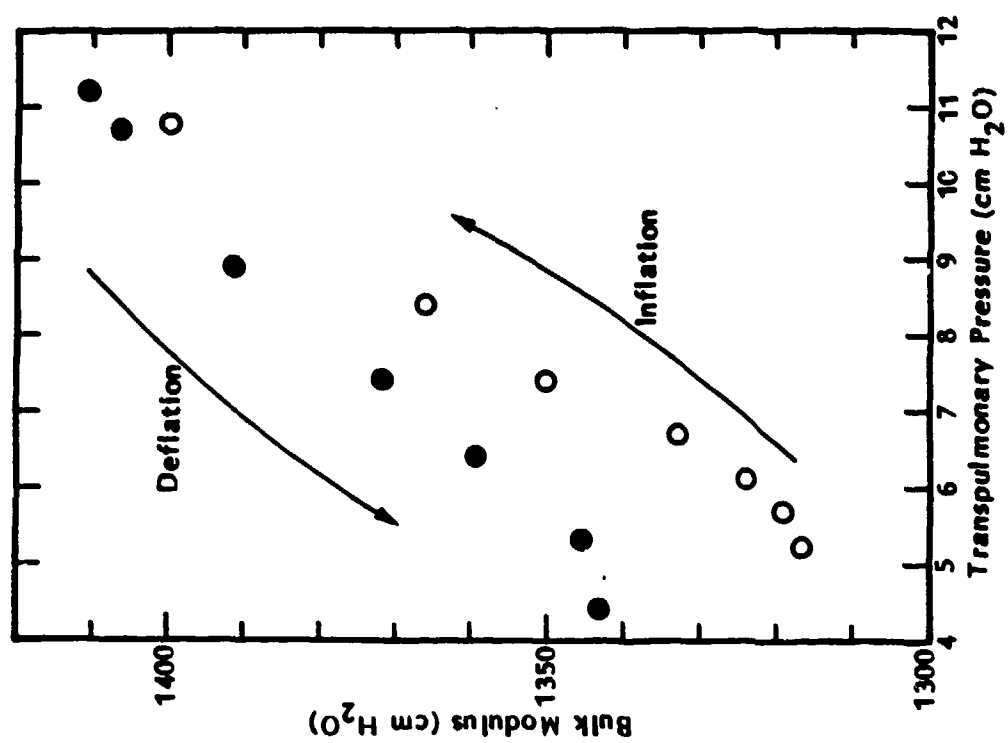


Figure 12. Bulk modulus of lung tissue and bulk modulus of whole lung.

lung are dominated by its composite nature. The results of the indentation tests showed that the ratio  $G_0/K_0$  varies from 0.3 to 0.5 depending on species and transpulmonary pressure.

The non-elastic nature of material cannot be described by a few parameters because there is an almost endless variety of ways that real material can deviate from the elastic ideal. One of the most important deviations is the dependence of the material constants on the history of the stresses that have been applied--these are called "memory" effects. These effects can be most clearly seen by applying sudden stresses or strains and observing how rapidly the system adjusts. The "creep test", for example, measures how long it takes a material to stretch when a load is suddenly applied. Almost immediately the material is pulled to a length at which the elastic forces balance the applied force, but over a longer period of time the material stretches even more before reaching a final length. This behavior can be characterized by an additional contribution to the elastic moduli that is created by the application of the external load, but which dies away with time. Tests of tissue properties, showed that this addition could be as much as 50% of the elastic component and last a few tenths of a second. See Figure 13. Tests were not devised to determine if similar memory effects exist for whole lung, which have elastic moduli that are one or two orders of magnitude larger than their tissue counterparts.

#### THORACIC RESPONSE

To the finite element model described in the previous section it is necessary to provide values for the seven material parameters for each of the four body material chosen to represent the thorax. Those parameters can be summarized by the relations

$$\text{Mass density} = \rho$$

$$\text{Bulk modulus} = K_0 + K_1 * \exp(-t/\lambda)$$

$$\text{Shear modulus} = G_0 + G_1 * \exp(-t/\beta)$$

Only a few of the 28 parameters have been measured directly, so before elaborate tests were devised and performed, calculations were made to determine which of the parameters are important to predicting and understanding the data

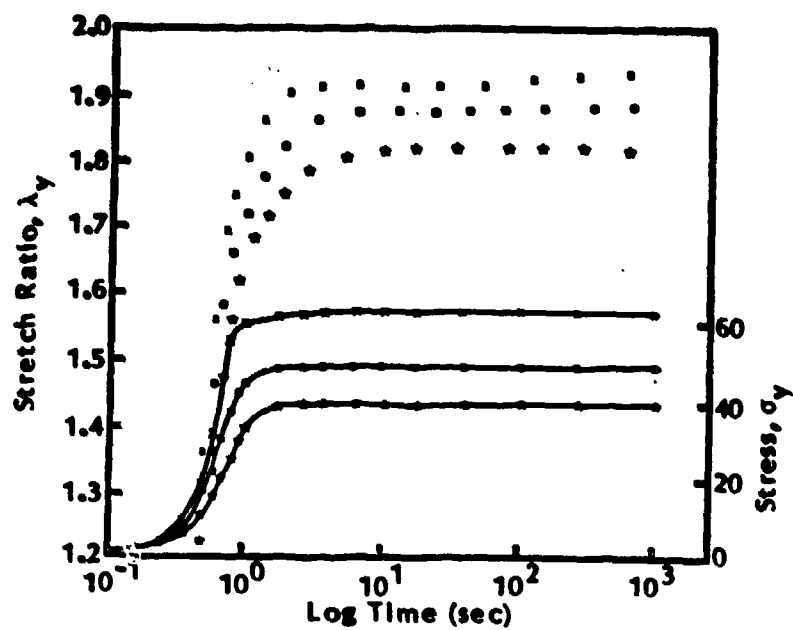


Figure 13. Suddenly applied stresses were used to determine viscoelastic properties.

currently available, that is, intrathoracic pressure time histories. Data from a particular field test was chosen to be the basis of comparison. In this test an animal was exposed to two blast waves separated by about 7 msec. Each parameter of the model was varied systematically and in combination with others, and the predictions compared with the measured data.

The results can be summarized as follows. None of the viscoelastic parameters ( $K_1$ ,  $\lambda$ ,  $G_1$ , or  $\beta$ ) had significant influence on the predicted ITP. Any differences observed were small compared with the deviation of the prediction from measurement and were small compared with the effects of varying other parameters. Next, it was found that the elastic properties of the rib and heart elements had little effect on the predictions provided they were chosen reasonably close (within a few orders of magnitude) to the known physiological values. The mass density of the rib, muscle, and heart are well known and reasonable variations (tens of percent) was not significant. The only truly sensitive parameters were the mass density and bulk modulus of the lung, which have been well measured in the experiments described earlier, and the effective shear modulus of the muscle layer. See Figure 14(a) for a summary.

It was mentioned earlier that one approximation introduced by a two-dimensional representation is that out-of-plane forces, such as those due to the rib cage, cannot be mechanistically modeled. If the shear modulus of muscle,  $G_0=10^4$ , were used in the model, the model would predict unnaturally large distortions and produce ITP results completely unlike measurement. See Figure 14b. If, on the other hand, the muscle layer is assigned an shear modulus that will give the two-dimensional chest the kind of stiffness actually observed, then the ITP predictions are much more reasonable. This parameter can be determined through experiments measuring the displacement of the chest wall under loading.

With the material parameters determined, comparison was made with field test data for sheep exposure to blast. For each case, the measured free-field blast wave was translated into a loading distribution based on the findings of the torso tests and calculations. When multiple blasts were involved, the loading was simply repeated at the appropriate time interval.

Organ	Parameter						
	$\rho$	$K_0$	$K_1$	$\lambda$	$C_0$	$C_1$	$\beta$
Lung	Sensitive	Sensitive	Can be neglected	Can be neglected	Can be neglected	Can be neglected	Can be neglected
Rib	Insensitve in physiological range	Insensitve in physiological range	Can be neglected	Can be neglected	Insensitve in physiological range	Can be neglected	Can be neglected
Muscle	Insensitve in physiological range	Insensitve in physiological range	Can be neglected	Can be neglected	Sensitive	Can be neglected	Can be neglected
Heart	Insensitve in physiological range	Insensitve in physiological range	Can be neglected	Can be neglected	Insensitve in physiological range	Can be neglected	Can be neglected



Sensitive



Insensitve in physiological range



Can be neglected

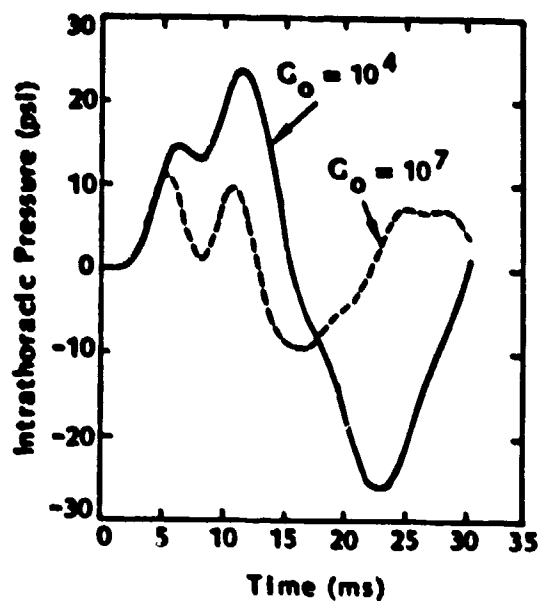


Figure 14. Sensitivity studies have shown which material properties are important for gross motion and ITP.

Figure 15 compares prediction and measurement for a 16 lb TNT charge that produced a single peak blast wave with a peak pressure of about 12 psi. The agreement is considered to be within the uncertainty of the blast conditions, instrument response, and particular animal anatomy. Similar results were obtained for other single blast conditions. After the initial peak, the predictions show continuing reverberation that arises from not including damping processes in the material description.

Figure 16 compares the results for an exposure to two blast waves with peak pressure of 40 psi separated in time by 7.6 msec---this was the case used in the sensitivity study. The agreement is also good, although the reverberation is more pronounced. The peaks are rounded off due to the finite spatial size of the elements and the negative phase is significantly overpredicted because constant material properties are being used.

Figure 17 compares the results for the same two intensity waves separated by a slightly longer time of 9.7 msec. The peaks are significantly underpredicted and the negative phases overpredicted. The initial blast wave in the previous two tests were identical, yet the measured response differed by almost a factor of three! Until the uncertainty in the test results is removed, it is difficult to assess the absolute accuracy of the model predictions for these high peak pressure exposures.

The dominant feature of the calculated lung pressure distribution is the propagation and reflection of relatively slow waves, predicted by the model to be about 30 m/sec. This phenomena arises in the model because of the combination of highly compressible, yet moderately dense lung material. In a parallel effort in Professor Fung's laboratory at UCSD, the propagation of parenchyma waves due to direct blast exposure was observed and measured. The results varied somewhat with species and transpulmonary pressure, but fell in a range about 30 m/sec. See Figure 18. These results not only support the qualitative nature of the model predictions, but confirms that the dominant material properties for describing lung dynamics are contained in the mass density and the elastic bulk modulus.

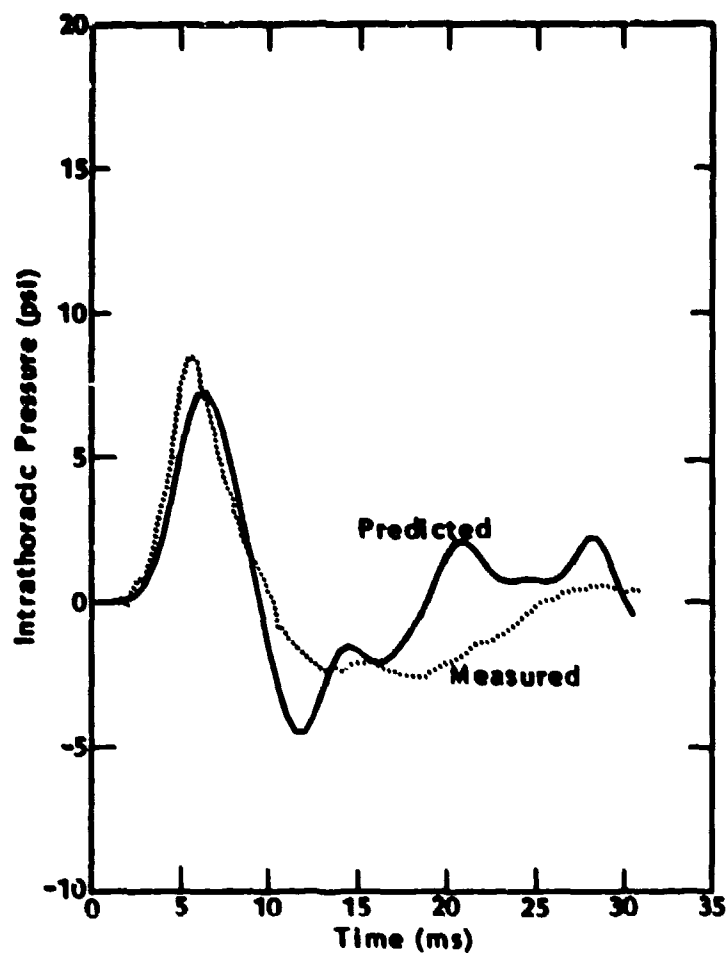


Figure 15. Comparison of predicted intrathoracic pressure and measured esophageal pressure for a single peak blast due to a 16 lb TNT charge.

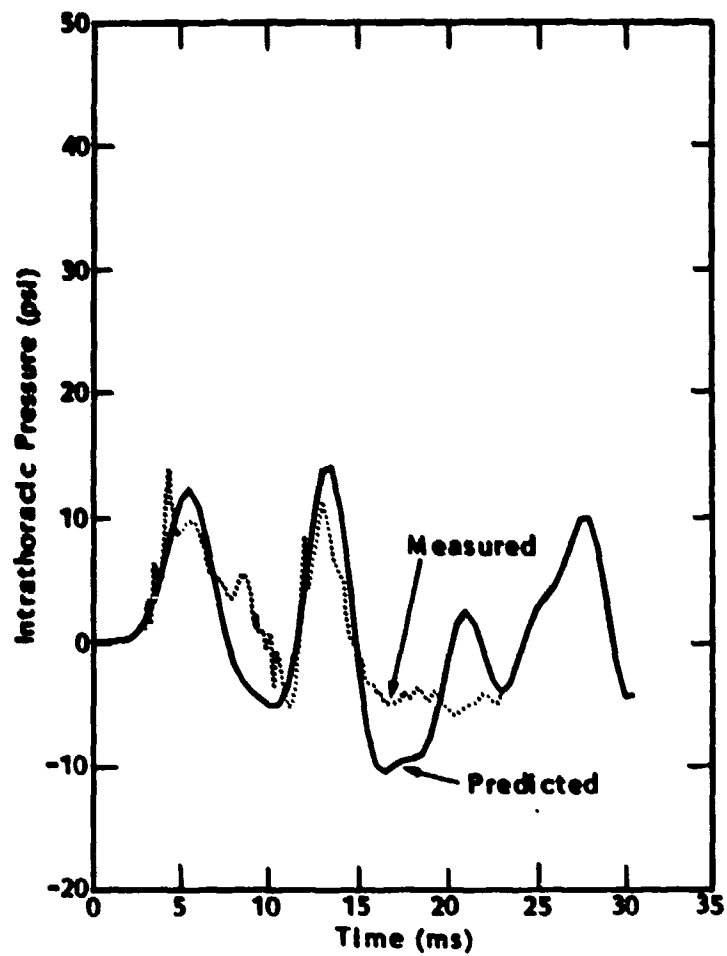


Figure 16. Comparison of predicted intrathoracic pressure and measured esophageal pressure for an exposure to two 40 psi blast waves separated in time by 7.6 msec.



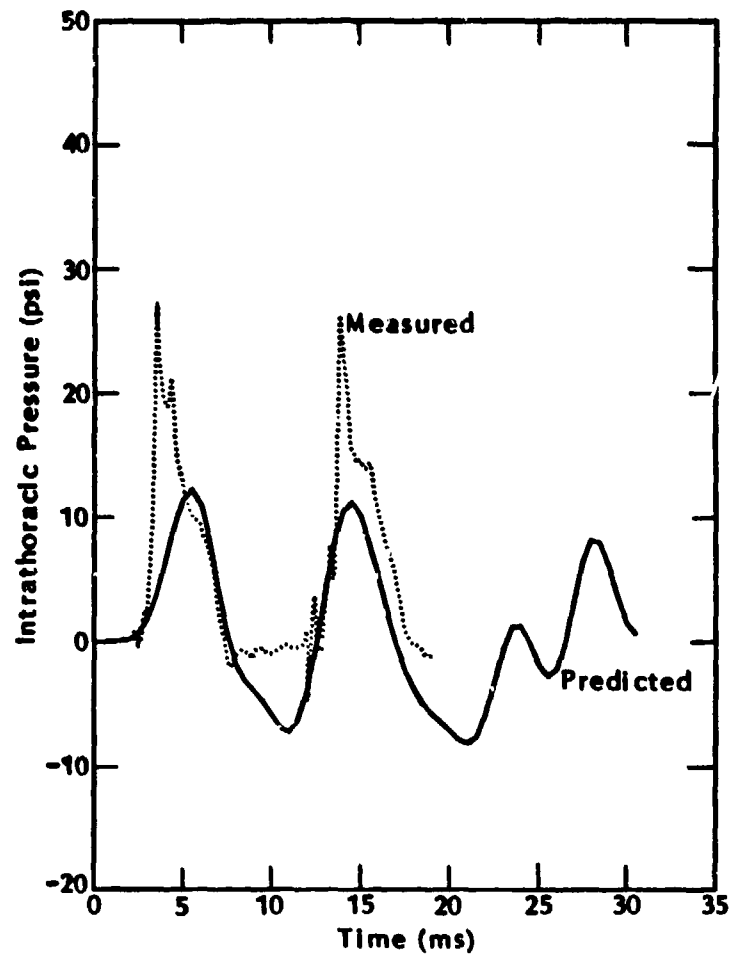


Figure 17. Comparison of predicted intrathoracic pressure and measured esophageal pressure for an exposure to two 40 psi blast waves separated in time by 9.7 msec.

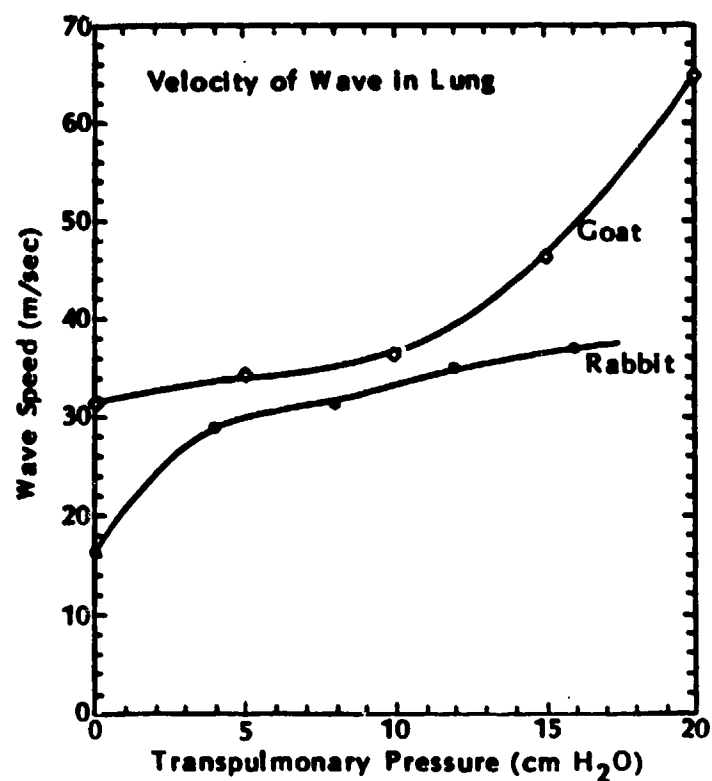


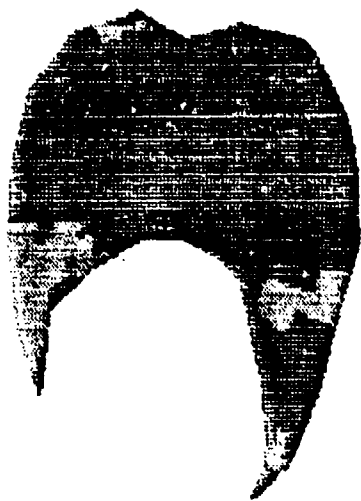
Figure 18. Dynamic loading on one side of the lung produced direct measurement of wave speed.

## LUNG INJURY MECHANISMS

It is a tenet of the bioengineering approach that when local stresses exceed the material strength of the tissue, damage will result. Although the injury mechanism is not known at this time, if the principle is valid, there should be a correlation between locations of stress concentration and injury sites. Figure 19a shows the distribution of predicted maximum stress (tension and compression) throughout the lung as a result of a typical blast loading. The largest stresses occur in specific locations: the pleural surfaces facing the blast and on the opposite side, at the boundaries with the heart, in the tips of the lobes, and at the geometric center where wave focusing occurs. The observed injury in a sheep lung is shown in Figure 19b after exposure to an intense blast. The red marks of hemorrhage are seen in the same general areas where stress concentration occurred. There has not been a quantitative comparison of local injury with local stress concentration but it seems likely that a correlation does exist.

Another feature of pleural injury is a banded hemorrhage pattern that has been called "rib marking," although it has not been established by direct measurement whether the marks correspond to the location of the ribs or the intracostal spaces. In an attempt to understand their origin, model calculations were made for an idealized section of the thorax containing rib, intracostal space, and a section of lung tissue. A compression wave was propagated into this local region, reflecting off the rib structure. The results showed that the difference in material density caused the local tension concentration to be higher under the bone, a difference that may be responsible for the rib markings observed. Carefully instrumented tests are required to confirm this prediction.

As a first step in quantifying the injury process and in assigning a threshold level for injury-causing stress, a novel experiment was devised by Professor Fung's group at UCSD. An apparatus was developed that allows the change of weight of a perfused lung to be determined with great accuracy. The experiment begins with an excised, perfused lung being maintained under stable, isogravimetric conditions. The lung is then directly subjected to a blast-like pressure wave or a local impact and the weight of the lung monitored. A threshold level of injury, measured by weight gain, is clearly



Tension



Compression

DISTRIBUTION OF PREDICTED MAXIMUM STRESS CONCENTRATIONS

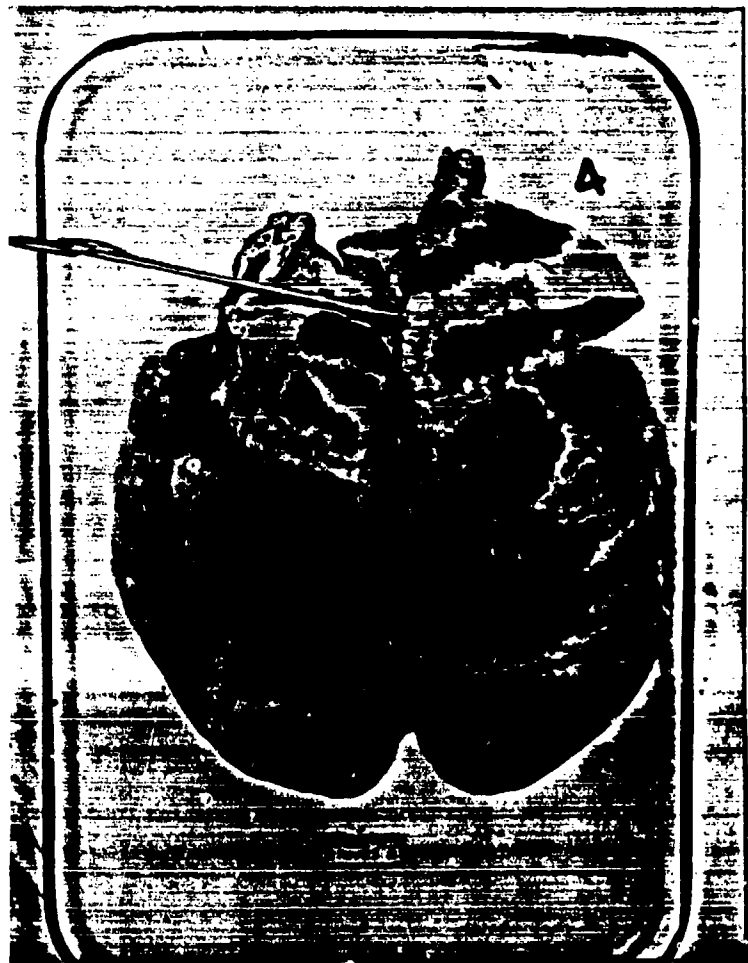


Figure 19. Observed distribution of injury.



**Tension**



**Compression**

**DISTRIBUTION OF PREDICTED MAXIMUM STRESS CONCENTRATIONS**



**Figure 19. Observed distribution of injury.**

noticed. See Figure 20. For example, pressure waves whose peak (as measured by a face-on probe) are less than 2.0 psi result in no net weight gain, implying that there has been no rupture of the vascular system. Conversely, as the peak pressure increases beyond 2.0 psi the rate of weight gain increases rapidly. Although the trauma is introduced in a manner that is not equivalent to that received by a lung in vivo, the evidence for a threshold level of local mechanical stress is strong.

Despite the qualitative agreement between the distribution and pattern of predicted stress and observed damage, the goal of the project is to provide a quantitative means for anticipating injury. The final mechanistic connection will require more study, however, a correlation has already been observed in field tests, relating peak ITP measurements to the severity of lung injury. Thus, if ITP could be reliably predicted, a correlation with damage could be based upon these observations.

In the previous section, we showed that the ITP time histories could be reasonably well predicted for single peak cases. WRAIR conducted a series of tests in which sheep were exposed to single blast waves of constant, positive impulse, as measured by a side-on pressure gauge. By varying the test conditions, a range of peak pressure and duration combinations were achieved. The tests showed that the maximum ITP varied with the peak pressure, despite the fact that the waves were iso-impulse, and that the severity of injury increased with the maximum ITP. The finite element model produced the same qualitative trend as the data. See Figure 21. In contrast, the lumped parameter model indicates that peak ITP is nearly constant over the pressure range.

This result is the most encouraging evidence that blast injury can be predicted using an engineering model. The prediction is dependent on the entire causal chain described in the Introduction. First, based on the torso study, the loading on the body increases as the peak pressure of the wave increases. Next, the stress in the lung is amplified by the slow wave speed of the parenchyma. Finally, the location of the esophageal measurement corresponds to a geometric focusing point of the compression waves.

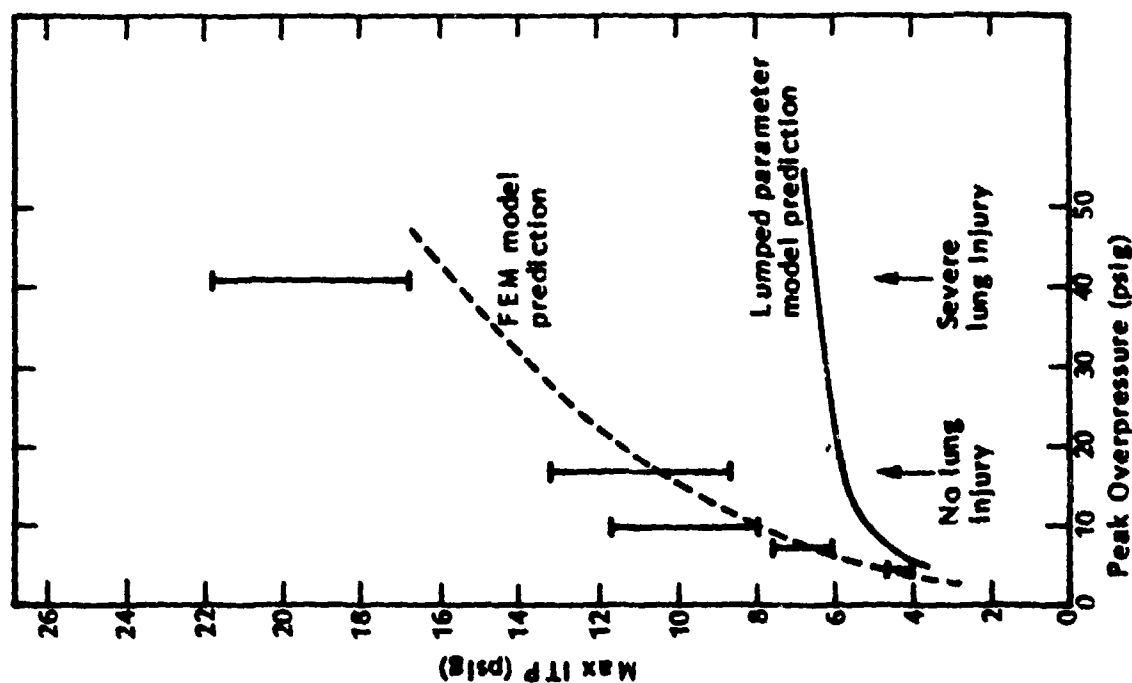
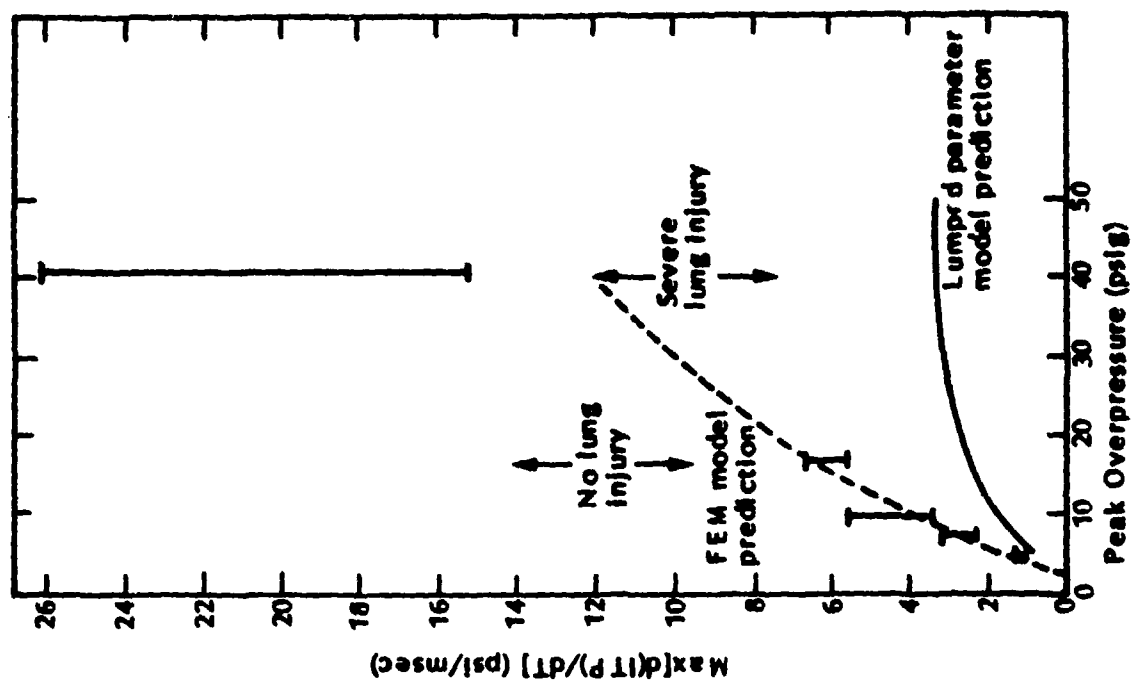


Figure 20. Iso-impulse study comparison of the FEM model prediction with WRAIR experimental results.

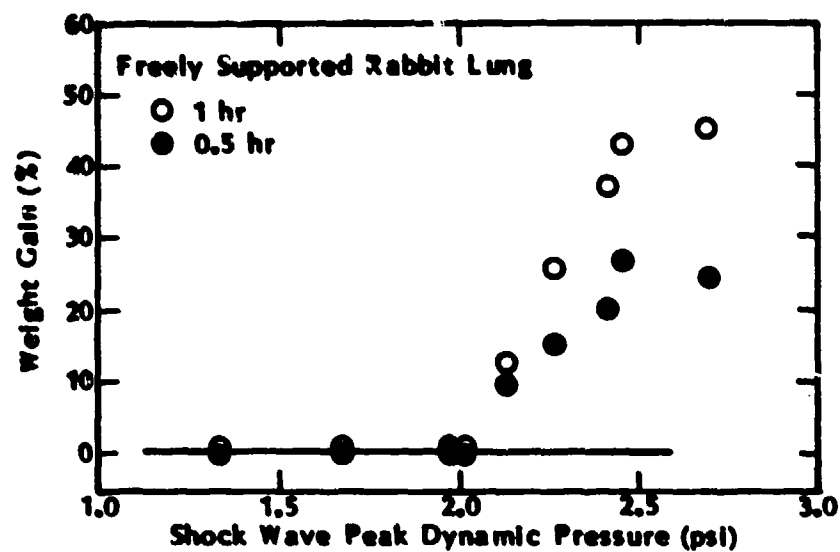


Figure 21. Weight gain in an isolated lung increases rapidly where the peak pressure of a directly applied blast wave exceeds 2.0 psi.



## EFFECTS OF CLOTHING

Field tests, using animals and human volunteers, showed that peak intra-thoracic pressure increased when the test subjects wore thick, ballistic jackets. Similar trends were seen by Clemenson when rabbits were wrapped in spongy covering, leading to the speculation that a temporal redistribution of the loading may produce better mechanical coupling with the body. Laboratory tests were conducted to determine the modification to loading caused by clothing. The data showed that peak pressure increased with the thickness of the clothing layer.

Calculations made with the cross-sectional finite element model of the sheep, modified to include a layer of compliant material with the same geometric and physical properties of the ballistic jacket, showed increased ITP response. The magnitude of the increase is about the same as that observed in field studies.

# **DISTRIBUTION LIST**

12 copies

Director  
Walter Reed Army Institute of Research  
Walter Reed Army Medical Center  
ATTN: SGRD-UWZ-C  
Washington, DC 20307-5100

1 copy

Commander  
US Army Medical Research and Development Command  
ATTN: SGRD-RMI-S  
Fort Detrick, Frederick, MD 21701-5012

12 copies

Defense Technical Information Center (DTIC)  
ATTN: DTIC-DDAC  
Cameron Station  
Alexandria, VA 22304-6145

1 copy

Dean  
School of Medicine  
Uniformed Services University of the Health Sciences  
4301 Jones Bridge Road  
Bethesda, MD 20814-4799

1 copy

Commandant  
Academy of Health Sciences, US Army  
ATTN: AHS-CDM  
Fort Sam Houston, TX 78234-6100